Investigation of molecular and elemental species dynamics in NTO, TNT, and ANTA using femtosecond LIBS technique

Sunku Sreedhar, E. Nageswara Rao, G. Manoj Kumar,[a] Surya P. Tewari, S. Venugopal Rao[*]

Advanced Centre of Research in High Energy Materials **(ACRHEM),**
University of Hyderabad, Prof. C. R. Rao Road,
Gachibowli, Hyderabad 500046, India
*, [a] Authors for correspondence: **svrsp@uohyd.ernet.in**; **manojsp@uohyd.ernet.in**

Abstract

We present results from the elemental and molecular species dynamics of high energy materials (HEMs) studied using laser induced breakdown spectroscopy with femtosecond (fs) laser pulses. Spectral emission behavior of atomic and molecular species of HEMs such as NTO (3-nitro-l,2,4-triazol-5-one), TNT (tri-nitro toluene) and ANTA (5-amino-3-nitro-1H-1,2,4-triazole) were studied in different atmospheres of Argon, Nitrogen, and ambient air. We used fs pulses (~40 fs, 2.5 mJ, 1 kHz) for creating the breakdown. CN and C_2 molecular species were formed from these organic molecules during the breakdown. These molecular species are key signatures of organics substances for identification of HEMs.

Introduction

Laser induced breakdown spectroscopy (LIBS), an emerging tool for multi-elemental analysis, has specific advantages compared to other techniques like Inductive Coupling Plasma Mass Spectrometry, Atomic Absorption Spectroscopy and Atomic Emission Spectroscopy [1-3]. A few noted advantages include simultaneous multi-element detection, high detection speed, requirement of small amount of material for testing, and material could be in any form. LIBS has been proved to be an attractive and versatile technique for the detection of hazardous and prohibited substances [5-9]. Especially, the standoff detection potential makes this technique an attractive contrivance for detection of high energy materials (HEMs)[5]. Introducing ultrashort pulses in LIBS has definite advantages [10], (a) low ablation threshold (b) less thermal damage to the sample (c) nearly background-free spectra devoid of Continuum and the possibility of beam filamentation over a period of few kilometers for implementing remote LIBS [11]. Femtosecond LIBS was successfully demonstrated for bacterial detection [12, 13], animal tissues [14], combustion diagnostics [15] and explosive detection too [16 -19].

High energy materials (HEM's) are soft organic compounds with the general formula $C_\alpha H_\beta N_\gamma O_\nu$. The dominant peaks in the LIBS spectra of all such compounds comprise of Carbon, Hydrogen, Oxygen and Nitrogen. They all are exhibit similar molecular and elemental signatures in their LIBS spectra. These molecular species are key signatures of organics substances for identification of organic HEMs [7, 8]. CN and C_2 molecular species were formed when these organic molecules underwent breakdown. The plasma chemistry involving the formation of molecular fragments is a complex phenomenon. The formation of molecular species will be either from the ejection of molecular radicals due to direct vaporization of sample or due to the recombination reaction happening between the constituent atomic species present in plasma. There could be the chances of surrounding atmosphere interacting with the plasma continents and leading to formation of these molecular radicals. Especially in the case of CN molecular fragments, the probability of CN formation is more when atmospheric nitrogen interacts with C and C_2. Therefore, it is necessary to study the sources for formation of CN and C_2 molecules. Very few studies are available in literature explaining the formation dynamics of CN species of plastics and graphite with ns produced plasmas [21-29]. Some research groups have performed studies explaining the temporal features of atomic and molecular species in HEMs [30]. In this paper we present the results of our recent efforts to study high energy materials (HEMs) using laser induced breakdown spectroscopy (LIBS) with ultrashort laser pulses. Spectral emission behavior of HEMs such as NTO (3-nitro-l,2,4-triazol-5-one), TNT (tri-nitro toluene) and ANTA (5-amino-3-nitro-1H-1,2,4-triazole)

were studied in different atmospheres like Argon, Nitrogen and ambient air. A precise kinetic study of molecular bands and elemental intensities evolving in time allowed us to distinguish the contribution of native CN bonds released by the sample and those formed due to Carbon recombination with atmospheric Nitrogen. The present work attempts to explain the sources of formation of these molecular fragments from HEMs samples under different surrounding atmospheres. Furthermore we attempt to explain the variation of these molecular formations observed in the aforementioned three atmospheres.

Experimental Setup

Amplified Ti:sapphire laser pulses with duration of ~40 fs, maximum energy of 2.5 mJ delivered at a repetition rate of 1 kHz (central wavelength of 800 nm) were used in all the experiments. The samples were made in the form of a pellet by first grinding the sample with agate mortar and then applying 10 ton hydraulic pressure onto the powdered sample. The fs laser pulses were focused on the target sample mounted on XY translation stage with 8 cm plano-convex lens. The energy used to produce plasma was ~1.2 mJ and corresponding fluence estimated was ~22 J/cm^2. Dense plasma was formed at the focal region. A collection lens system unit was placed to collect the light from plasma and light passed through a fiber optic cable and finally transferred to a gated ICCD spectrometer (Andor i-star DH734 ICCD + ME 5000 Mechelle spectrograph, resolution 5000). Argon and Nitrogen gases were purged through nozzle onto the sample where laser was focused onto the pellets. Three HEMs samples NTO ($C_2H_2N_4O_3$), TNT ($C_7H_5N_3O_6$) and ANTA ($C_2H_3N_5O_2$) were used in our studies for investigation of molecular emission with fs LIBS. All samples have same elements C, H, N and O with different composition. The structure and composition of three samples were presented in table 1.
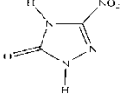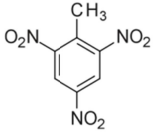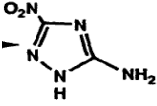
Sample	Composition	Nitro groups	Structure
NTO	$C_2H_2N_4O_3$	1	
TNT	$C_7H_5N_3O_6$	3	
ANTA	$C_2H_3N_5O_2$	1	

Table 1 Compositional and structural information of HEMs.

Results and Discussion

Figure 1 corresponds to LIBS spectra of TNT sample recorded in air atmosphere. The spectral peaks corresponding to a particular atom/molecular species have been assigned and are shown in the graph. We have observed the CN emission in three different regions corresponding to $B^2S_u^+ - X^2S_g^+$ states transitions. The transition with $\Delta v = 0$ were obtained in the 385-389 nm spectral range, transitions with $\Delta v = +1$ were found in the 414-422 nm spectral range and transition with $\Delta v = -1$ were observed in the 356-358 nm spectral range. The

C$_2$ swan band corresponding to states $D^3\Pi_g - A^3\Pi_u$ with transitions $\Delta\nu = 0$ was observed near 516.47 nm. Elemental peaks corresponding to C, H, N and O were also assigned and are shown in figure 1. The overall description of elemental and molecular peaks observed in the spectra from three samples is presented in table 2. All elemental and molecular features observed for three samples in three different atmospheres were not the same. Depending on the sample nature as well as surrounding atmosphere, slight variations in intensities were observed.
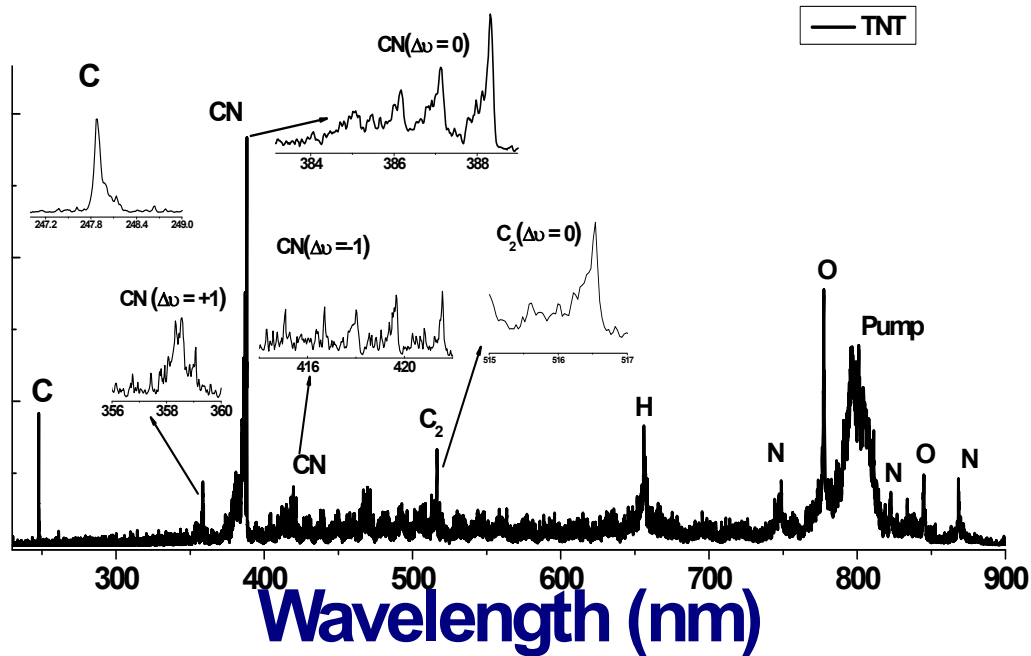

Figure 1 LIBS spectra of TNT obtained with fs laser excitation in air atmosphere, the gate width of 800 ns and 100 ns initial delay were utilized to record the spectra.

Species	Peaks (nm)
C	247.82
Ca	393.35, 396.83, 422.67
CN - ($\Delta\upsilon = +1$)	359.02
CN - ($\Delta\upsilon = 0$)	388.28, 387.07, 386.16, 385.40, 385.01
CN - ($\Delta\upsilon = -1$)	421.50, 419.63, 418.03, 416.78
C$_2$ - ($\Delta\upsilon = +1$)	473.63, 471.50
C$_2$ - ($\Delta\upsilon = 0$)	516.47
Na	588.89, 589.50
H$_\alpha$	656.2
O	777.2, 844.55
N	742.2, 744.1, 746.8, 821.50, 822.35, 867.80, 868.80

Table 2 Description of elemental and molecular peaks obtained with the spectra of NTO, TNT and ANTA samples in three atmospheres.

The surroundings of plasma influence the molecular formation significantly. Therefore, to study the sources of formation mechanism of CN and C_2 molecules, we have chooses three different atmospheres such that, one was nitrogen which created 100 % nitrogen surrounding the plasma, second was ambient air atmosphere where more than 75% was nitrogen. In the last case the experiments were performed in argon buffer gas (0% surrounding nitrogen), which is used to create inert atmosphere surrounding the plasma for demonstrating a situation for CN formation between the atoms present in the plasma only. We attempt to understand the CN molecular formation mechanism and figure out the contribution from surrounding atmosphere to the plasma. Experiments were performed in a controlled manner such that purging the gas on to the sample exactly where the plasma was formed. Figures 2(a) - 2(c) illustrate the spectra obtained with NTO, TNT and ANTA samples using fs pulses. In each case the top graph corresponds to the LIBS spectra obtained in Nitrogen whereas the middle spectra were obtained in argon atmosphere and the bottom spectra were obtained in Argon atmosphere.
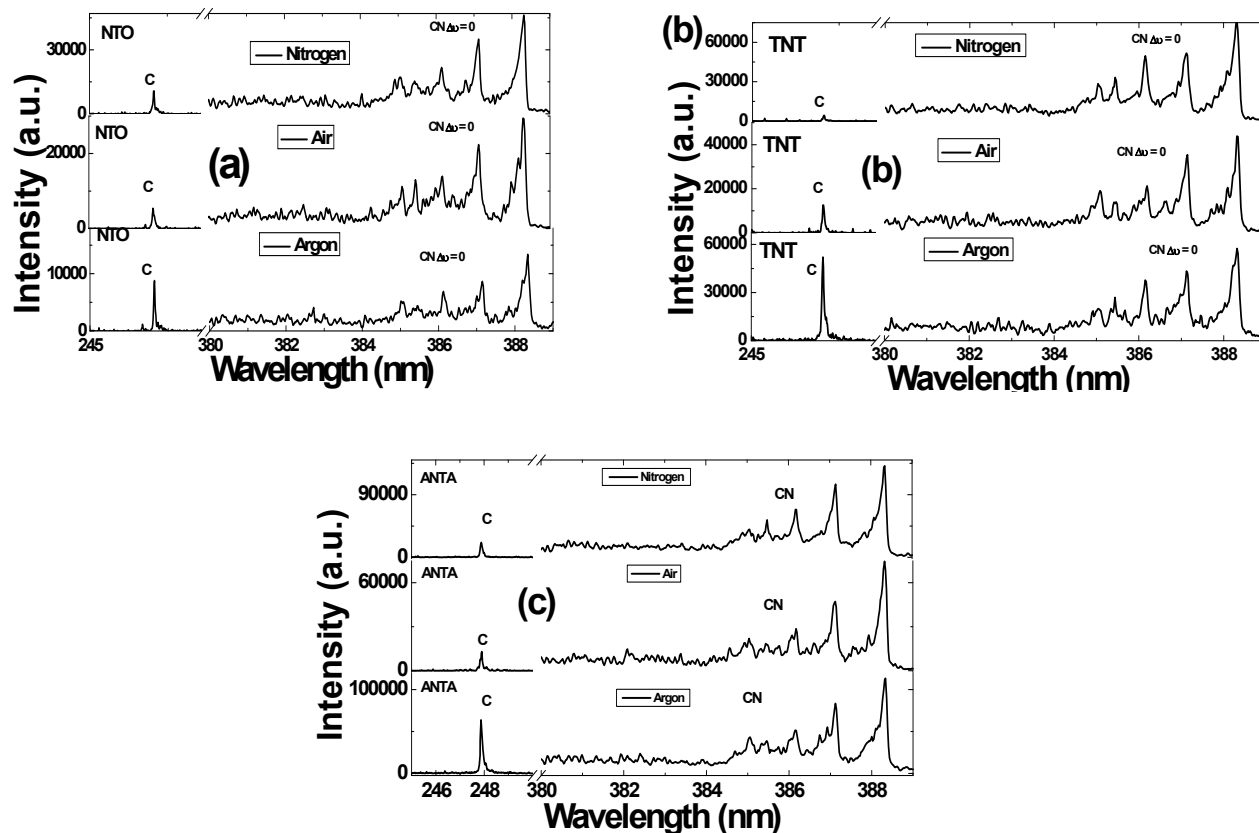

Figure 2(a) – (c) LIBS spectra of (a) NTO, (b) TNT and (c) ANTA obtained with fs laser excitation in three different atmospheres, the gate width of 800 ns and 100 ns initial delay were utilized to record the spectra.

CN violet band transitions with $\Delta v = 0$ were observed with greater magnitude among all but these peaks were intense in Nitrogen atmosphere in comparison to others. Carbon peak was observed to be higher in Argon atmosphere. In three atmospheres cases the availability of carbon is the same (since it is from sample only) but differ in the nitrogen content due to surrounding atmosphere. It is evident that elemental/molecular carbons in plasma react with nitrogen decreased as in the surrounding nitrogen percentage decreased which is reflected in CN magnitude. Similar observation was recorded in all three samples. It signifies that Nitrogen present in the ambient atmosphere plays a major role in CN molecular formation. In Argon atmosphere the surrounding nitrogen content is nil and, therefore, the un-reacted carbon will remain intact and precisely this is the reason Carbon peak was observed to be higher in Argon atmosphere. The C_2 swan band (transitions with $\Delta v = 0$ at 516.46 nm) was observed in TNT for all atmospheres and was observed to be weak in NTO and ANTA in Argon atmospheres.

Temporal studies

To understand the temporal dynamics of LIBS signal we had recorded spectra with different gate delays. The LIBS spectra were recorded with 25 ns gate width starting at 80 ns with 25 ns interval up to 400 ns. Figures 3 (a) – (d) present the typical intensity variation of different elemental and molecular species observed with time in ANTA sample, (a) corresponds to C-247.82 nm, (b) CN – 388.2 nm, (c) H – 656.2 nm and (d) N-868.8 nm sample for all three atmospheres. The intensity of C, H, N, O, and CN peaks recorded with time delay were fitted with a single exponential. Table 3 summarizes the decay constants obtained for all three samples in all all atmospheres. As seen from figures 3(a), (b) [decay of C-247.82 nm and CN -388.2 nm] the carbon intensity was observed to be high in argon atmosphere compared other two atmospheres. The CN intensity was observed to be high in Nitrogen atmosphere. From the decay constants presented in table 3 we notice that the Carbon decay constant was longer for Argon atmosphere and CN decay was longer for nitrogen atmosphere for all samples. In Argon atmosphere due to the lack of availability of surrounding nitrogen carbon will remain un-reacted. Hence the decay of carbon was slower in argon whereas in other atmospheres carbon will react with nitrogen present in the atmosphere and, therefore, the decay of carbon species is expected to be faster in Nitrogen and air atmosphere. The probability of CN species formation was high in air and nitrogen atmospheres due to the presence of surrounding nitrogen but it is limited in argon since there is no extra nitrogen content apart from sample. Consequently, the CN species decays very fast in the argon atmosphere. Hydrogen peak intensity was high in argon atmosphere for all the samples; the decay rate was also observed to be longer in argon atmosphere. The Oxygen peaks decay constants observed for three samples in argon demonstrated long decay time for NTO with similar behavior observed in air atmosphere too. We observed longer decay times of Oxygen and this could be due to the usually high plasma lifetime in argon atmosphere and, therefore, the elemental species life time will be higher.
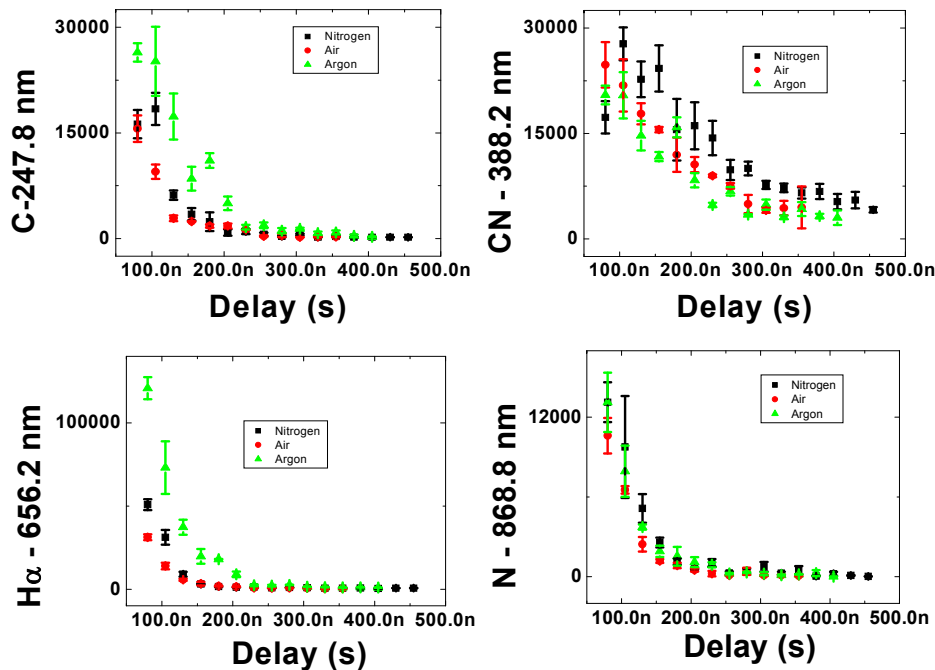

Figure 3 (a) – (d) decay of C-247.82, CN - 388.2, H-656.2 nm and N-868.8 nm peaks in three atmospheres for ANTA samples. Spectra were recorded with a gate width of 25 ns and step size of 25 ns, after an initial gate delay of 80 ns of laser pulse.

The CN band formation in laser produced plasmas is mainly governed by a set of chemical reactions taking place within the plasma and are described by $C_2 + N_2 \rightarrow 2\ CN$ (1) and $2C + N_2 \rightarrow CN$ (2) [20 – 25]. In the above reactions highest availability of N_2 will be from atmospheric air. Therefore, these reactions will be dominant when Nitrogen surrounds the plasma and contribute strongly towards the CN molecular formation. There are another

possible reactions contributing towards the formation of CN species, for e.g. $C_2 + N \rightarrow CN + C$ (3) and $C + N \rightarrow CN$ (4) [23 - 27]. These two reactions [(3) and (4)] refer to CN formation when N reacts with C_2 and C species. The possibility of these reactions arises only from Nitrogen presence in the sample constituents within the plasma.

Decay Constants				
Sample	Peak	Nitrogen (ns)	Air (ns)	Argon (ns)
NTO	C-247.2 nm	43	54	121
	CN – 388.2nm	209	172	164
	H- 656 nm	34	36	73
	O-777.2 nm	36	39	66
	N-868 nm	35	42	40
TNT	C-247.2 nm	45	65	106
	CN – 388.2nm	364	181	151
	H- 656 nm	36	37	58
	O-777.2 nm	39	38	74
	N-868 nm	45	35	34
ANTA	C-247.2 nm	41	32	71
	CN – 388.2nm	129	80	60
	H- 656 nm	24	30	47
	O-777.2 nm	30	33	38
	N-868 nm	42	32	40

Table 3 Summary of the decay constants of important atomic and molecular species extracted from the LIBS spectra of NTO, TNT and ANTA samples acquired using fs pulses

Figures 4(a)-4(c) represents the temporal variation in CN(tot)/C ratio for all the samples. Figure 4(a) illustrates that at initial time delays CN/C ratio for NTO increased slowly. After initial times (~150 ns) the ratio increased sharply in Nitrogen. But in Argon atmosphere it continued increasing slowly. It was observed in all samples that the CN/C ratio increased gradually (up to ~150 ns) in all atmospheres. It peaked at time scales of ~225 ns. As time progress the plasma tries to expand and while expanding the species present in the plasma try to interact with the surrounding atmosphere where the secondary chemical reactions take place. Hence, stronger CN molecular formation takes place where the above stated reactions are dominant at these time scales. All samples exhibited the increment of the CN/C ratio in air and nitrogen atmosphere. The CN/C ratio increment in argon atmosphere was not steep due to lack of additional nitrogen atoms to interact with the plasma. CN formation occurs with species present in the plasma only. At initial time scales CN could form from its native radicals and the chemical reaction occurring within the species present in the plasma only. At these time scales CN could form following reactions (3) and (4). As time progresses the plasma will expand and during this period the species present in the periphery of the plasma tries to interact with the surrounding atmosphere. In these time scales CN formation could be boosted by the probability of chemical reactions (1) and (2). By closely observing the temporal decay dynamics of all three samples it is evident that CN formation was stronger in air and nitrogen compared to argon thereby clearly suggesting the surrounding atmospheric effects on the molecular formation. Complete details of the temporal variation of various molecular and atomic species from HEMs samples under different surrounding atmospheres could possibly lead to better understanding of the sources of formation and thereby better techniques for identification (combined with other complementary data) of such materials.
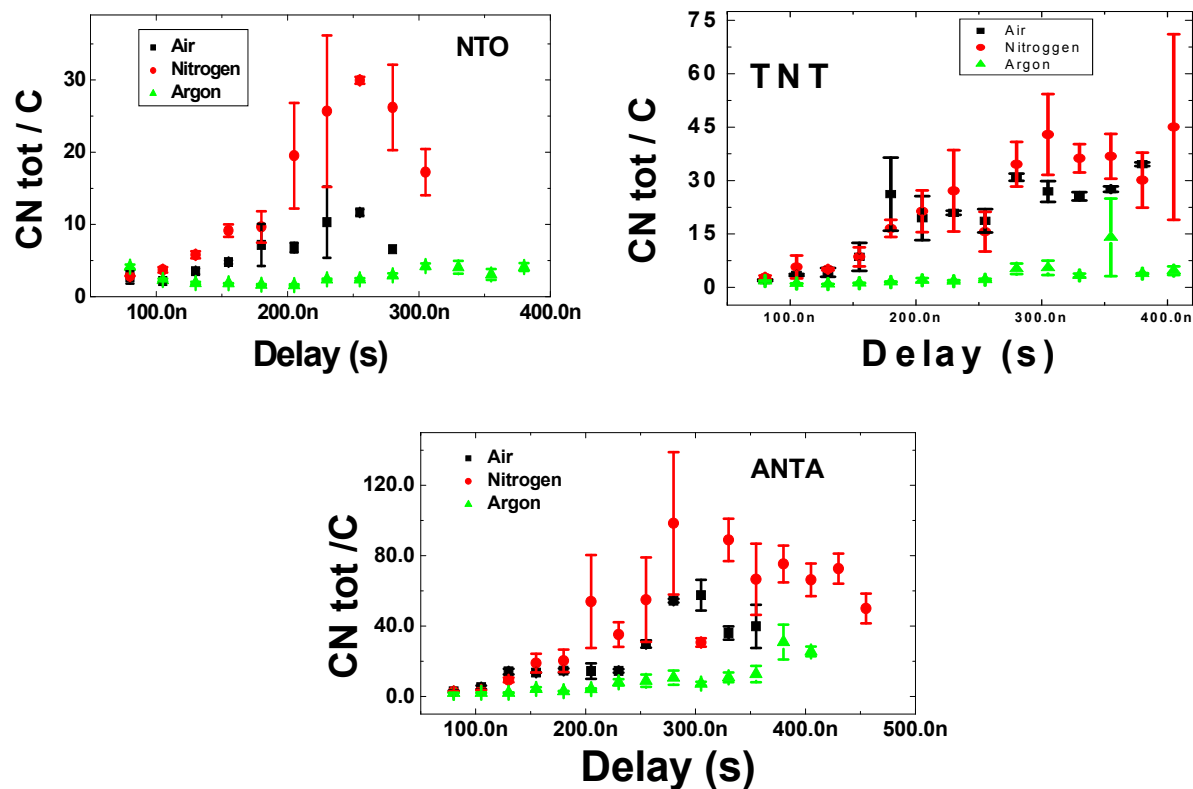
Figure 4 Temporal evolution of CN (388.2 nm)/C (247.8 nm) in (a) NTO (b) TNT and (c) ANTA. Spectra were recorded with a gate width of 25 ns and step size of 25 ns after an initial gate delay of 80 ns of laser pulse.

Conclusions

LIBS spectral features of three HEMs NTO, TNT and ANTA were studied in three different atmospheres Nitrogen, ambient air and Argon. The differences observed in elemental and molecular features in three atmospheres were discussed. Temporal variations of spectral studies were performed for all the samples. The C -247.8 nm decay observed to be longer in argon case compared to nitrogen and air. The CN molecular formation was observed more intense in nitrogen and air atmosphere compared to argon. The CN/C ratios has peaked ~200 ns – 275 ns range for the samples.

Acknowledgments

Financial support from DRDO, India is gratefully acknowledged. The authors also acknowledge the samples provided by HEMRL, Pune, India and P. Ravi, ACRHEM.

References

[1]   A.W. Miziolek, V. Palleschi, I. Schechter, eds., Laser-Induced Breakdown Spectroscopy (LIBS): Fundamentals and Applications, Cambridge Univ. Press, 2006.
[2]   J.P. Singh and S.N. Thakur, eds., *Laser-Induced Breakdown Spectroscopy* (Elsevier, 2007).
[3]   D.W. Hahn and N. Omenetto, Laser-Induced Breakdown Spectroscopy (LIBS), Part II: Review of Instrumental and Methodological Approaches to Material Analysis and Applications to Different Fields, Appl. Spectrosc. 66 (2012) 347-419.

[4]   M.A. Kumar, S. Sreedhar, S. Venugopal Rao, P. Prem Kiran, S.P. Tewari, G.M. Kumar, Laser induced breakdown spectroscopy-based investigation and classification of pharmaceutical tablets using multivariate chemometric analysis, Talanta. 87 (2011) 53-59.

[5]   C. López-Moreno, S. Palanco, J.J. Laserna, F.C. DeLucia Jr., A.W. Miziolek, J. Rose, R.A. Walters, A.I. Whitehouse, Test of a stand-off laser-induced breakdown spectroscopy sensor for the detection of explosive residues on solid surfaces, J. Anal. Atom. Spectrom. 21 (2006) 55-60.

[6]   J.L. Gottfried, F.C. De Lucia Jr., C.A. Munson, A.W. Miziolek, Standoff detection of chemical and biological threats using laser-induced breakdown spectroscopy, Appl. Spectrosc. 62 (2008) 353-363.

[7]   V. Lazic, A. Palucci, S. Jovicevic, C. Poggi, E. Buono, Analysis of explosive and other organic residues by laser induced breakdown spectroscopy, Spectrochim. Acta Part B. 64 (2009) 1028-1039.

[8]   P. Lucena, A. Doña, L.M. Tobaria, J.J. Laserna, New challenges and insights in the detection and spectral identification of organic explosives by laser induced breakdown spectroscopy, Spectrochim. Acta Part B. 66 (2011) 12–20.

[9]   K. Sovova, K. Dryahina, P. Spaneˇl, M. Kyncl and S. Civis, A study of the composition of the products of laser-induced breakdown of hexogen, octogen, pentrite and trinitrotoluene using selected ion flow tube mass spectrometry and UV-Vis spectrometry, Analyst 135 (2010) 1106-1114.

[10]   E.L. Gurevich, R. Hergenroeder, Femtosecond laser-induced breakdown spectroscopy: physics, applications, and perspectives, Appl. Spectrosc. 61 (2007) 233A-242A.

[11]   Ph. Rohwetter, J. Yu, G. Me´jean, K. Stelmaszczyk, E. Salmon, J. Kasparian, J.-P. Wolf, L. Wo¨ste, Remote, LIBS with ultrashort pulses: characteristics in picosecond and femtosecond regimes, J. Anal. At. Spectrom. 19 (2004) 437–444.

[12]   M. Baudelet, L. Guyon, J. Yu, J.-P. Wolf, T. Amodeo, W. Frejafon, P. Laloi, Femtosecond time-resolved laser-induced breakdown spectroscopy for detection and identification of bacteria: A comparison to the nanosecond regime, J. Appl. Phys. 99 (2006) 84701-9.

[13]   M. Baudelet, J. Yu, M. Bossu, J. Jovelet, J.-P. Wolf, T. Amodeo, E. Frejafon, and P. Laloi, Discrimination of microbiological samples using femtosecond laser-induced breakdown spectroscopy, Appl. Phys. Lett. 89 (2006) 163903.

[14]   D. Santos, R.E. Samad, L.C. Trevizan, A.Z. de Freitas, N.D. Vieira, and F.J. Krug, Evaluation of Femtosecond Laser-Induced Breakdown Spectroscopy for Analysis of Animal Tissues, Appl. Spectro. 62 (2008) 1137-1143.

[15]   M. Kotzagianni and S. Couris., Femtosecond laser induced breakdown for combustion diagnostics, Appl. Phys. Lett. 100 (2012) 264104-4.

[16]   Y. Dikmelik, C. McEnnis, and J. B. Spicer, Femtosecond and nanosecond laser-induced breakdown spectroscopy of trinitrotoluene, Opt. Exp. 16 (2008) 5332-5337.

[17]   Y. Dikmelik, C. McEnnis, J.B. Spicer, Femtosecond laser-induced breakdown spectroscopy of explosives, Proc. SPIE. 6217II (2006) 62172A.

[18]   F.C. De Lucia, J.L. Gottfried, A.W. Miziolek, Evaluation of femtosecond laser-induced breakdown spectroscopy for explosive residue detection, Opt. Exp. 17 (2009) 419-425.

[19]   S. Sreedhar, G. Manoj Kumar, M. Ashwin Kumar, P. Prem Kiran, Surya P. Tewari, S. Venugopal Rao, Femtosecond and nanosecond laser induced breakdown spectroscopic studies of NTO, HMX, and RDX, Spectrochim. Acta Part B (2012) 79–80 (2013) 31–38.

[20]   Jesu´ s Anzano, Roberto-Jesu´ s Lasheras , Beatriz Bonilla, Justiniano Casas, "Classification of polymers by determining of C1:C2: CN: H: N: O ratios by laser-induced plasma spectroscopy (LIPS)", Polymer Testing, 27, 705–710, (2008).

[21]   S.S. Harilal, Riju C. Issac, C.V. Bindhu, Pramod Gopinath, V.P.N. Nampoori, C.P.G. Vallabhan, "Time resolved study of CN band emission from plasma generated by laser irradiation of graphite", Spectrochimica Acta Part A 53 (1997) 1527-1536.

[22]   A. Kushwaha, R.K. Thareja, Dynamics of laser ablated plasma: formation of C_2 and CN, Appl. Opt. 47 (31) (2008) G65 – G71.

[23]   J. Sun, H. Feng, J. Gan, Q. Li, K. Gao 1, N. Xu, Z.F. Ying, J.D. Wu, Reactive expansion of laser-induced boron/carbon plasma in ECR Nitrogen plasma during the deposition of BCN films, Diamond & Related Materials 21 (2012) 66–72.

[24]   D. Ding, P. Liang, J. Wu, N. Xu, Z. Ying, J. Sun, A comparative study of the enhancement of molecular emission in a spatially confined plume through optical emission spectroscopy and probe beam deflection measurements, Spectrochim. Acta B (2012). 79–80 (2013) 44–50

[25]   S. Grégoire, V. Motto-Ros, Q.L. Ma, W.Q. Lei, X.C. Wang, F. Pelascini, F. Surma, V. Detalle, J. Yu, Correlation between native bonds in a polymeric material and molecular emissions from the laser-induced plasma observed with space and time resolved imaging, Spectrochim. Acta Part B 74–75 (2012) 31–37

[26]   M. Dong, X. Mao, J.J. Gonzalez, J. Lu, R.E. Russo. Time resolved LIBS of Atomic and molecular carbon form Coal in air, Argon and helium, J. Anal. At. Spectrom. **27** (2012) 2066-2075.

[27]   M. Dong, J. Lu, S. Yao, Z. Zhong, J. Li, J. Li, W. Lu, Experimental study on the characteristics of molecular emission spectroscopy for the analysis of solid materials containing C and N, Opt. Exp. 19 (2011) 17021-17029

[28]   Q. Ma, P.J. Dagdigian, Kinetic model of atomic and molecular emissions in laser-induced breakdown spectroscopy of organic compounds, Anal. Bioanal. Chem. 400 (2011) 3193-3205.

[29]   P.J. Dagdigian, A. Khachatrian, V.I. Babushok, Kinetic model of C/H/N/O emissions in laser-induced breakdown spectroscopy of organic compounds, Appl. Opt. 49 (2010) C58-C66.

[30]   V.I. Babushok, F.C. DeLucia Jr., P.J. Dagdigian, J.L. Gottfried, C.A. Munson, M.J. Nusca, A.W. Miziolek, Kinetic modeling study of the laser-induced plasma plume of cyclotrimethylenetrinitramine (RDX), Spectrochim. Acta B. 62 (2007) 1321-1328.